PHARMACEUTICS, PREFORMULATION AND DRUG DELIVERY

Crystal Structure Determination of Mebendazole Form A Using High-Resolution Synchrotron X-Ray Powder Diffraction Data

FABIO FURLAN FERREIRA,[1] SELMA GUTIERREZ ANTONIO,[2] PAULO CÉSAR PIRES ROSA,[3] CARLOS DE OLIVEIRA PAIVA-SANTOS[2]

[1]Laboratório Nacional de Luz Síncrotron, Caixa Postal 6192, CEP: 13083-970, Campinas, SP, Brazil

[2]Depto. de Físico-Química, Instituto de Química, Universidade Estadual Paulista, Caixa Postal 355, CEP: 14801-970, Araraquara, SP, Brazil

[3]Depto. de Química Analítica, Instituto de Química, Universidade Estadual de Campinas, Caixa Postal 6154, CEP: 13084-862, Campinas, SP, Brazil

Received 18 June 2009; accepted 13 July 2009

Published online 4 August 2009 in Wiley InterScience (www.interscience.wiley.com). DOI 10.1002/jps.21902

ABSTRACT: The crystal structure determination of mebendazole form A, an anthelmintic drug, was performed for the first time by applying the DASH software program to synchrotron X-ray powder diffraction data, and supported by a satisfying Rietveld fit. This polymorph of mebendazole crystallizes in a triclinic ($P\bar{1}$) space group, with unit-cell parameters $a = 5.5044(2)$ Å, $b = 11.2872(2)$ Å, $c = 12.5276(5)$ Å, $\alpha = 66.694(2)^\circ$, $\beta = 82.959(2)^\circ$, $\gamma = 78.443(2)^\circ$, $V = 699.52(5)$ Å^3, $Z = 2$, $M = 295.293\,\mathrm{g\,mol^{-1}}$, $\rho_{calc} = 1.4021\,\mathrm{g\,cm^{-3}}$, and $\rho_{meas} = 1.3935(66)\,\mathrm{g\,cm^{-3}}$, which were obtained by means of the unit-cell formula weight and a picnometric measurement, respectively. The goodness-of-fit and R-factors were, respectively: $\chi^2 = 1.746$, $R_F^2 = 1.69\%$, $R_{wp} = 5.72\%$, and $R_p = 4.37\%$. A weak nonclassical hydrogen bond involving the atoms N(3)–H(23)···O(11) may be responsible for the greater stability of the polymorphic form A of mebendazole due to the strongest electronegativity of nitrogen. © 2009 Wiley-Liss, Inc. and the American Pharmacists Association J Pharm Sci 99:1734–1744, 2010

Keywords: X-ray powder diffractometry; crystal structure; polymorphism; crystallography; *ab initio* calculations; quantitative phase analysis; synchrotron; mebendazole; polymorph A; anthelmintic drug

INTRODUCTION

Mebendazole (MBZ), IUPAC name (5-benzoyl-1*H*-benzimidazole-2-yl)-carbamic acid methyl ester ($C_{16}H_{13}N_3O_3$, $M = 295.293\,\mathrm{g\,mol^{-1}}$, chemical structure shown in Fig. 1), is a benzimidazole drug used in the treatment of infestations by worms including pinworms, roundworms, tapeworms,

Correspondence to: Fabio Furlan Ferreira (Telephone: 55-19-3512-1285; Fax: 55-19-3512-1004; E-mail: ffurlanf@gmail.com)

Journal of Pharmaceutical Sciences, Vol. 99, 1734–1744 (2010)

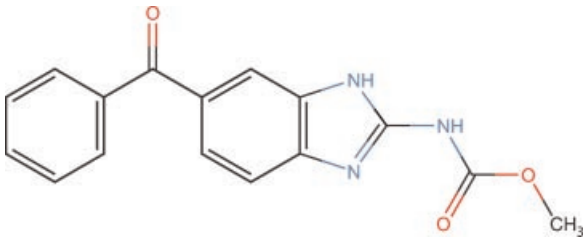

Figure 1. Chemical structure of mebendazole.

hookworms, and whipworms.[1] It causes slow immobilization and death of the worms by selectively and irreversibly blocking uptake of glucose and other nutrients in susceptible adult intestine where these helminthes reside.[1] Also, it disrupts cellular reproduction by affecting the protein threads which connect the centromere regions of chromosomes.[1]

MBZ presents three polymorphic forms (A, B, and C) displaying significant different solubility and therapeutic effects, all being practically insoluble in water.[2,3] Also, it is known that the polymorphic form C is the most efficacious one[4,5] in spite of the fact that the most soluble one, the polymorph B, perhaps due to possible toxicity of this form.[6–8] Besides the fact the polymorphic form A is the least soluble and the most stable one, there are several recommendations that the maximum amount of it should not be greater than 30% in the formulation.[4] Due to this characteristic, it is important to identify and/or quantify its presence in the tablets of mebendazole. Also, owing to the difficulties in obtaining single crystals, the complete crystal structure data of pure MBZ polymorphs are hard to obtain.[5] Mebendazole hydrobromide, which crystallizes in a monoclinic space group ($P2_1/c$),[9] mebendazole hydrochloride, a new stable salt obtained from recrystallization of forms A, B, and C of MBZ in diverse solvents with the addition of hydrochloric acid solution, which crystallizes in an orthorhombic space group ($Cmc2_1$),[5] and MBZ propionic acid, a 1:1 molecular complex, that crystallizes in a triclinic space group ($P\bar{1}$),[10] are some of the forms of mebendazole described in the literature. Very recently, the crystal structure of the polymorph C of mebendazole was determined by single-crystal X-ray diffraction studies.[11]

Several techniques have been used to identify the polymorphic forms of mebendazole, infrared spectroscopy being one of the most commonly employed.[6,12] The demonstration of differing structures by means of single-crystal X-ray diffraction is currently regarded as definitive evidence of polymorphism. However, X-ray powder diffraction can also be used to provide unequivocal proof of polymorphism.[13] Among others, these are the prerequisite techniques for the structural characterization of pharmaceutical polymorphs.[13]

In this work, high-resolution synchrotron X-ray powder diffraction data and a simulated annealing algorithm [14–16] were used to determine the crystal structure of the polymorphic form A of mebendazole which, as far as we are aware, has never before been reported. The final refinement of the structure was performed by the Rietveld method,[17] which was also used to perform a quantitative phase analysis of a sample containing both the polymorphs A and C.

EXPERIMENTAL

High-resolution synchrotron X-ray powder diffraction data were collected at the X-ray Powder Diffraction (D10B – XPD) beamline[18] of the Brazilian Synchrotron Light Laboratory (LNLS, Campinas, SP, Brazil) placed after a dipole magnet source. X-rays of $\lambda = 1.24014$ Å wavelength were selected by a double-bounce Si(1 1 1) monochromator with water cooling for the first crystal, while the second one is bent for sagittal focusing.[19] The wavelength and the zero point were determined from several reflections of the SRM640c silicon standard. The beam was vertically focused in the sample's position by a bent Rh-coated ultra-low-expansion glass mirror placed before the monochromator, which also provides filtering of high-energy photons (third- and higher-order harmonics), with a resulting spot size of ~1 mm (vertical) × ~2 mm (horizontal) at the sample position. The experiments were performed in the vertical scattering plane, that is, perpendicular to the linear polarization of the incident photons. The diffracted beam was analyzed using a Ge(1 1 1) single crystal and detected using an NaI(Tl) scintillation counter with a pulse-height discriminator in the counting chain. The incoming beam was also monitored by a scintillation counter to normalize the decay of the primary beam.

The powder sample, as acquired from Formil Química Ltda. (Jandira, SP, Brazil, lot number FMB.04.121140.27), was loaded into a 0.7-mm diameter borosilicate glass capillary and data were recorded at room temperature for ~5 s at

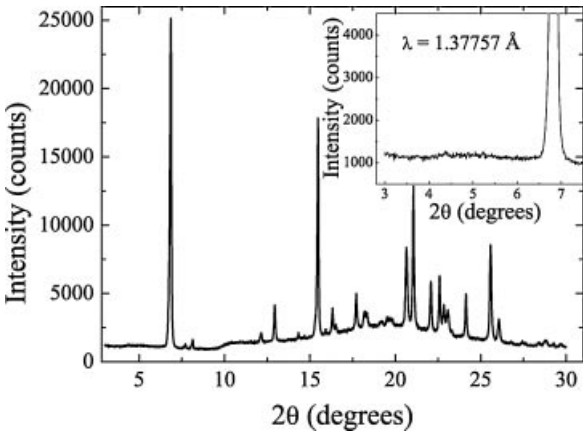

Figure 2. X-ray powder diffractogram of mebendazole form A, obtained with $\lambda = 1.37757$ Å. No peaks of polymorph C were observed, as shown in the inset, where the most intense peak of polymorph C lies.

each 2θ in steps of 0.008° from 5.5° to 32.012°. It should be mentioned that prior the final measurement, a rapid initial scan (not shown) was performed starting at 4° (2θ) in order to verify if other reflections were present, fact that was not observed. A measurement performed on the same beamline using the aforementioned high-resolution setup, but with a $\lambda = 1.37757$ Å wavelength, was carried out on the sample of polymorph A of mebendazole used for the crystal structure determination, in order to highlight the absence of polymorph C, as shown in Figure 2. Another sample, containing both the polymorphs A and C, in order to quantify their fractions, was also measured.

A BOMEM MB-100 infrared spectrophotometer was used to certify that the sample provided by Formil Química Ltda. refers to the polymorph A of mebendazole.[20]

RESULTS

The DASH software program[14] was used for both indexing, by using an internal version of the *DICVOL91* software program,[21] and crystal structure determination using synchrotron X-ray powder diffraction data. The first 15 peaks were individually fit, yielding the following values for a triclinic space group ($P1$ or $P\bar{1}$): $F(15) = 264.8$, $M(15) = 102.0$, $a = 12.52629$ Å, $b = 11.29012$ Å, $c = 5.50575$ Å, $\alpha = 78.430^\circ$, $\beta = 97.070^\circ$, $\gamma = 113.310^\circ$, and $V = 699.73$ Å^3.

Alternatively, the peak profiles were manually fit using the CMPR[22] software program in order to generate a list of peak positions and areas (33 peaks were fit) to serve as an input file for the Crysfire suite of auto-indexing programs.[23,24] The highest figure-of-merit (M)[25] was obtained using the KOHL software program[26] implemented into Crysfire and yielded the following values for a triclinic space group ($P1$ or $P\bar{1}$): $I(20) = 20$, $M(20) = 39.53$, $a = 11.2908$ Å, $b = 12.5240$ Å, $c = 5.5076$ Å, $\alpha = 97.051^\circ$, $\beta = 101.548^\circ$, $\gamma = 66.661^\circ$, and $V = 699.791$ Å^3.

Although the unit-cell values obtained by the two methods differ, they represent the same solution and can be easily exchanged by a transformation matrix.[27] The transformation matrix, from the solution obtained by the DASH software to the Crysfire suite is:

$$T = \begin{pmatrix} 0 & -1 & 0 \\ 1 & 0 & 0 \\ 0 & 0 & -1 \end{pmatrix}$$

After the unit-cell parameters have been roughly evaluated, a Pawley fit,[28] implemented into the DASH software program, was performed on unit-cell parameters, zero point of the detector and background terms, yielding the following values: $a = 12.5237$ Å, $b = 11.2854$ Å, $c = 5.5015$ Å, $\alpha = 78.458^\circ$, $\beta = 97.025^\circ$, $\gamma = 113.285^\circ$, $V = 698.97$ Å^3, and Pawley $\chi^2 = 6.35$, under a triclinic $P1$ space group. Those values were then used in conjunction with the chemical structure available in the DrugBank database,[29] card number DB00643, in the process of crystal structure determination by means of a simulated annealing algorithm.[15,16] Estimating that the molecular volume accommodates two molecules, fifteen runs of the simulated annealing process were globally optimized and the best result was then considered in the final refinement of the structure. In the process of crystal structure determination, the molecular positions and orientations as well as any flexible torsion angles that may be present, also known as the degrees of freedom of the system, were adjusted to the experimental data. During the simulated annealing process, the full range of possible values were allowed to vary.[14] According to David et al.,[14] the two most obvious indicators of a successful structure solution are a visual assessment of the goodness of fit between the experimental and simulated powder pattern and the ratio "profile χ^2/Pawley χ^2," which should

generally be less than 5.[14] In the present case, the ratio was $10.39/6.35 \cong 1.6$.

In order to check the consistency of the obtained results for space group choice, unit-cell parameters, bond distances, angles and torsions, the PLATON software program was used.[30] The ADDSYM routine detected that there was a (pseudo) center of symmetry, indicating that the correct space group would be $P\bar{1}$ instead of $P1$. As in the triclinic space group the unit-cell axes dimensions have to be presented with values going from the lowest to the highest, the reduced unit-cell parameters[31] were converted as being: $a = 5.505$ Å, $b = 11.289$ Å, $c = 12.531$ Å, $\alpha = 66.70°$, $\beta = 82.96°$, $\gamma = 78.44°$, and $V = 699.9$ Å^3. In this case, the transformation matrix to the new cell and the origin shift to the centrosymmetric one were, respectively:

$$T = \begin{pmatrix} 0 & 0 & 1 \\ 0 & 1 & 0 \\ -1 & 0 & 0 \end{pmatrix}$$

and 0.4355, 0.0911, −0.0770.

It should be mentioned that the choice of $P1$ as a starting space group, although having twice the number of parameters being varied in order to find the solution as well as being much more time consuming it would be easily turn into $P\bar{1}$ space group, as it was the case. Otherwise, if we started with $P\bar{1}$, and the solution was found in $P1$, the whole procedure should be repeated, demanding much more time. It is important to mention that the final solution was found in less than one computing day.

The General Structure Analysis System (GSAS)[32] software program and its graphical user interface, EXPGUI,[33] were then used to perform a Rietveld refinement.[17] Prior to the final refinement, a Le Bail fit[34] with subsequent calculation of the unit-cell parameters was performed. The background was fit using a 10-term Chebyschev polynomial. The peak profile was modeled by a pseudo-Voigt profile function as parameterized by Thompson et al.[35] with low-angle asymmetry corrections by Finger et al.[36] and microstrain anisotropic broadening terms by Stephens.[37]

Having obtained the unit-cell parameters as well as the profile terms, which were not allowed to vary during the initial Rietveld refinement cycles, a script written by Wright,[38] available at the CCP14 website, was used to restrain both the bond distances and angles in weights of 0.05 Å and 2.0°, respectively, during the Rietveld refinement. Also, soft planar group restraints were applied to

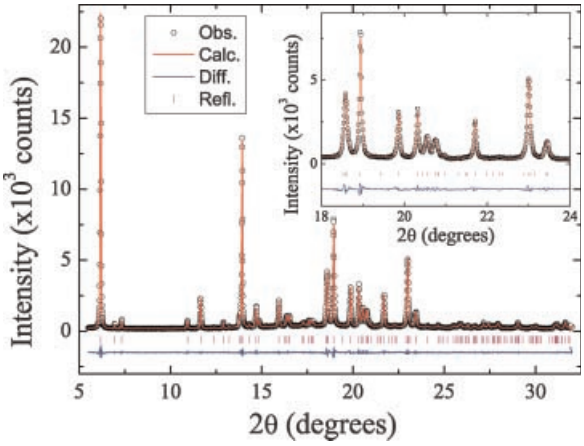

Figure 3. Rietveld refinement of mebendazole form A: measured pattern (circles), calculated pattern (solid line), and difference profile (bottom solid line). Tick marks (|) at the bottom of the pattern indicate peak positions allowed by the unit-cell parameters and space group. The inset presents a magnified region of the diffractogram.

the phenyl and benzimidazole rings. The initial overall bond, angle and planar group restraints weights were fixed in 10,000, 1000, and 1000, respectively, and were decreased until 1 during the final refinement cycles. When the refinement appeared to be stable, all parameters (scale factor, background terms, unit cell, profile, structural, and spherical harmonics, to account for possible preferred orientation of the crystals) were refined, converging to an excellent fit, which is shown in Figure 3. Atomic dislocation parameters for hydrogen atoms were kept as being twice of those of C, N, and O, which were constrained to be equal.

The final refined values for the unit-cell parameters after the Rietveld fit were: $a = 5.5044(2)$ Å, $b = 11.2872(2)$ Å, $c = 12.5276(5)$ Å, $\alpha = 66.694(2)°$, $\beta = 82.959(2)°$, $\gamma = 78.443(2)°$, $V = 699.52(5)$ Å^3, $\rho_{calc} = 1.4021$ g cm^{-3}, and $\rho_{meas} = 1.3935(66)$ g cm^{-3}, which were obtained by means of the unit-cell formula weight and a picnometric measurement, respectively, and $Z = 2$. The goodness-of-fit indicators and R-factors,[39] R_F^2, R_{wp}, and R_p, were, respectively: $\chi^2 = 1.746$, $R_F^2 = 1.69\%$, $R_{wp} = 5.72\%$, and $R_p = 4.37\%$. The Durbin–Watson statistic,[40] which is a test for autocorrelation, and, in GSAS, indicates that no serial correlation in fit at 90% confidence would occur for $1.979 < DWd < 2.021$, was $DWd = 1.304$. It indicates that the standard uncertainties (s.u.) obtained are underestimated. CCDC 736731 contains the supplementary crystallographic data

Table 1. Structural Atomic Parameters Obtained after the Rietveld Refinement

Name	x	y	z	$U_{iso}/U_e \times 100$
N(1)	−0.8089(38)	0.0778(14)	0.0529(17)	1.66(34)
C(2)	−0.9375(45)	0.1810(16)	−0.0241(21)	1.66(34)
N(3)	−0.8737(41)	0.2908(13)	−0.0223(20)	1.66(34)
H(23)	−0.963(15)	0.3818(25)	−0.061(10)	3.3(7)
C(4)	−0.5600(38)	0.3204(14)	0.0939(20)	1.66(34)
C(5)	−0.3822(45)	0.2487(17)	0.1741(22)	1.66(34)
C(6)	−0.3426(38)	0.1111(18)	0.2174(23)	1.66(34)
C(7)	−0.4469(44)	0.0447(15)	0.1722(22)	1.66(34)
C(8)	−0.6257(42)	0.1181(17)	0.0917(25)	1.66(34)
C(9)	−0.6915(38)	0.2509(18)	0.0593(23)	1.66(34)
H(24)	−0.641(11)	0.4126(37)	0.0851(71)	3.3(7)
H(25)	−0.200(15)	0.0547(40)	0.2697(89)	3.3(7)
H(26)	−0.426(15)	−0.0545(21)	0.2107(96)	3.3(7)
C(10)	−0.2316(44)	0.3159(17)	0.2168(14)	1.66(34)
O(11)	−0.1859(26)	0.4231(12)	0.1468(11)	1.66(34)
C(12)	−0.1360(39)	0.2646(22)	0.3371(13)	1.66(34)
C(13)	0.0362(42)	0.3182(20)	0.3693(17)	1.66(34)
C(14)	0.0799(32)	0.2863(22)	0.4857(21)	1.66(34)
C(15)	−0.0453(43)	0.1939(23)	0.5705(13)	1.66(34)
C(16)	−0.2248(44)	0.1472(24)	0.5382(18)	1.66(34)
C(17)	−0.2637(38)	0.1741(26)	0.4250(20)	1.66(34)
H(27)	0.102(14)	0.3981(70)	0.3106(64)	3.3(7)
H(28)	0.235(15)	0.3082(90)	0.5068(56)	3.3(7)
H(29)	0.004(14)	0.155(12)	0.6552(22)	3.3(7)
H(30)	−0.322(10)	0.0841(92)	0.6021(52)	3.3(7)
H(31)	−0.409(18)	0.1397(92)	0.4090(57)	3.3(7)
N(18)	−1.1119(31)	0.1792(14)	−0.0914(18)	1.66(34)
H(32)	−1.201(18)	0.105(11)	−0.046(12)	3.3(7)
C(19)	−1.2498(56)	0.2898(13)	−0.1666(29)	1.66(34)
O(20)	−1.2263(32)	0.4011(12)	−0.1802(16)	1.66(34)
O(21)	−1.3970(34)	0.2656(11)	−0.2170(15)	1.66(34)
C(22)	−1.5544(23)	0.3670(16)	−0.2982(13)	1.66(34)
H(33)	−1.615(24)	0.3228(56)	−0.3507(85)	3.3(7)
H(34)	−1.715(16)	0.4015(77)	−0.2513(56)	3.3(7)
H(35)	−1.449(8)	0.4432(43)	−0.3533(93)	3.3(7)

Atoms labeling are indicated by "atom", fractional coordinates (x, y, and z), and isotropic atomic displacement (U_{iso}/U_e) parameters are also shown.

for this paper. These data can be obtained free of charge from The Cambridge Crystallographic Data Centre via www.ccdc.cam.ac.uk/data_request/cif.

Table 1 shows the structural atomic parameters obtained after the Rietveld refinement. Bond distances and bond angles are shown in Table 2. Torsion angles are shown in Table 3. Intra- and intermolecular hydrogen bonds are displayed in Table 4. Least-squares planes calculation performed by PLATON[30] on a 5-membered ring system, on two 6-membered ring systems and on a 9-membered ring system is presented in Table 5.

DISCUSSION

The crystal structure of MBZ form A is comprised by one molecule in the asymmetric unit, shown in Figure 4 as an ORTEP-3 drawing.[41] Due to the fact that all atoms lie in general positions, the multiplicity of the $P\bar{1}$ space group generates two molecules per unit cell. Each of these molecules is intermolecularly connected on opposite sides of the same imidazole ring by hydrogen bonds, displayed in Table 4, involving the atoms N(3)–H(23)···O(11) and N(18)–H(32)···N(1). The latter forms an infinite chain along the (110) plane, as can be seen in Figure 5a. Figure 5b displays the intra- and intermolecular H-bonds.

Also presented in Table 4, an intramolecular hydrogen bond is observed between the atoms N(3)–H(23)···O(20). This intramolecular bond closes a chelating 6-membered ring system composed by O(20)–C(19)–N(18)–C(2)–N(3)–H(23) atoms. The highest deviation from the least-squares plane passing through this ring is 0.13(8) Å for H(23) (root mean square error (r.m.s.e.) of contributing atoms is 0.020 Å), indicating an almost planar system. In comparison to the recently published crystal structure of the polymorph C of mebendazole,[11] a very good agreement can be seen.

According to the results presented in Table 5, all rings are almost planar. The most deviating atom of the 9-membered ring, the imine nitrogen (N(1)) of the benzimidazole group, is distorting the whole ring due to its characteristic of acceptor atom on a strong intermolecular hydrogen bond with the nitrogen atom (N(18)) of the carbamate moiety. Differently to what was recently reported for the crystal structure of the polymorph C of mebendazole,[11] which shows a weak nonclassical hydrogen bond involving the atoms C(6)–H(6)···O(2), a weak hydrogen bond in the present case is observed between the atoms N(3)–H(23)···O(11). This bond may be responsible for the greater stability of the polymorphic form A of mebendazole due to the strongest electronegativity of nitrogen. What is more, the torsion angle C(4)–C(5)–C(10)–O(11) = −33(3)° is taking the carbonyl group of the benzoyl moiety out of plane. A closer inspection of the torsion angle O(11)–C(10)–C(12)–C(13) = −12(3)° reveals that the carbonyl group is noncoplanar with the phenyl ring. A least-squares analysis of the deviation of O(11) atom from the phenyl (0.75(2) Å) and benzimidazole (−0.63(1) Å) planes explains their nonplanar character. The movement of the benzoyl part of

Table 2. Bond Lengths (Å) and Bond Angles (°) of Mebendazole Form A

N(1)–C(2)	1.318(11)
N(1)–C(8)	1.392(11)
C(2)–N(3)	1.363(11)
C(2)–N(18)	1.361(12)
N(3)–H(23)	0.997(13)
N(3)–C(9)	1.400(11)
C(4)–C(5)	1.379(11)
C(4)–C(9)	1.378(11)
C(4)–H(24)	1.015(13)
C(5)–C(6)	1.407(11)
C(5)–C(10)	1.493(11)
C(6)–C(7)	1.341(11)
C(6)–H(25)	1.024(13)
C(7)–C(8)	1.388(11)
C(7)–H(26)	1.017(13)
C(8)–C(9)	1.371(11)
C(10)–O(11)	1.234(11)
C(10)–C(12)	1.505(10)
C(12)–C(13)	1.394(11)
C(12)–C(17)	1.399(11)
C(13)–C(14)	1.396(11)
C(13)–H(27)	1.014(13)
C(14)–C(15)	1.388(10)
C(14)–H(28)	1.023(13)
C(15)–C(16)	1.375(12)
C(15)–H(29)	1.023(13)
C(16)–C(17)	1.362(12)
C(16)–H(30)	1.014(13)
C(17)–H(31)	1.026(13)
N(18)–H(32)	0.99(15)
N(18)–C(19)	1.373(11)
C(19)–O(20)	1.232(11)
C(19)–O(21)	1.216(11)
O(21)–C(22)	1.412(10)
C(22)–H(33)	1.085(13)
C(22)–H(34)	1.094(12)
C(22)–H(35)	1.090(13)
H(33)–H(34)	1.776(12)
H(33)–H(35)	1.774(12)
H(34)–H(35)	1.83(5)
C(19)–O(21)–C(22)	122.7(1.7)
C(2)–N(1)–C(8)	110.9(1.5)
C(2)–N(3)–C(9)	109.2(1.3)
C(2)–N(18)–C(19)	121.9(1.9)
N(1)–C(2)–N(3)	107.3(1.3)
N(1)–C(2)–N(18)	126.3(1.7)
N(3)–C(2)–N(18)	126.4(1.5)
C(5)–C(4)–C(9)	116.9(1.3)
C(4)–C(5)–C(6)	120.6(1.4)
C(4)–C(5)–C(10)	120.9(1.4)
C(6)–C(5)–C(10)	118.4(1.3)
C(5)–C(6)–C(7)	122.1(1.2)
C(6)–C(7)–C(8)	117.2(1.5)
N(1)–C(8)–C(7)	132.6(1.7)
N(1)–C(8)–C(9)	106.1(1.1)
C(7)–C(8)–C(9)	121.3(1.4)
N(3)–C(9)–C(4)	131.8(1.6)
N(3)–C(9)–C(8)	106.4(1.3)
C(4)–C(9)–C(8)	121.8(1.1)
O(11)–C(10)–C(5)	117.4(1.3)
O(11)–C(10)–C(12)	116.2(1.7)
C(5)–C(10)–C(12)	126.1(1.4)
C(10)–C(12)–C(13)	124.7(1.4)
C(10)–C(12)–C(17)	116.5(1.5)
C(13)–C(12)–C(17)	117.4(1.2)
C(12)–C(13)–C(14)	122.4(1.2)
C(13)–C(14)–C(15)	118.4(1.2)
C(14)–C(15)–C(16)	118.3(1.2)
C(15)–C(16)–C(17)	123.3(1.3)
C(12)–C(17)–C(16)	120.1(1.3)
O(20)–C(19)–O(21)	124.0(3.0)
O(20)–C(19)–N(18)	124.0(3.0)
O(21)–C(19)–N(18)	111.2(1.9)
C(2)–N(3)–H(23)	125.0(1.8)
C(9)–N(3)–H(23)	126.0(2.0)
C(2)–N(18)–H(32)	106.0(9.0)
C(19)–N(18)–H(32)	116.0(9.0)
C(5)–C(4)–H(24)	124.0(2.0)
C(9)–C(4)–H(24)	119.0(2.0)
C(5)–C(6)–H(25)	124.0(3.0)
C(7)–C(6)–H(25)	114.0(3.0)
C(6)–C(7)–H(26)	120.0(2.0)
C(8)–C(7)–H(26)	123.0(2.0)
C(12)–C(13)–H(27)	121.0(2.0)
C(14)–C(13)–H(27)	117.0(1.9)
C(13)–C(14)–H(28)	122.0(2.0)
C(15)–C(14)–H(28)	120.0(2.0)
C(14)–C(15)–H(29)	121.0(2.0)
C(16)–C(15)–H(29)	120.0(2.0)
C(15)–C(16)–H(30)	119.0(2.0)
C(17)–C(16)–H(30)	118.0(2.0)
C(12)–C(17)–H(31)	123.0(2.0)
C(16)–C(17)–H(31)	117.0(2.0)
O(21)–C(22)–H(33)	104.0(5.0)
O(21)–C(22)–H(34)	108.0(4.0)
O(21)–C(22)–H(35)	109.0(4.0)
H(33)–C(22)–H(34)	109.0(7.0)
H(33)–C(22)–H(35)	109.0(7.0)
H(34)–C(22)–H(35)	117.0(6.0)

the molecule is consistent to what was previously reported for mebendazole hydrobromide[9] and mebendazole form C,[11] although it differs in direction and absolute values.

In order to check if the geometry of the obtained crystal structure was pertinent, a calculation of intramolecular bond distances and angles using MOGUL[42] was performed (Fig. 6). Only two bond distances were reported as "unusual": C(19)–

Table 3. Torsion Angles (°) of Mebendazole Form A

C(9)–N(3)–C(2)–N(18)	179(2)
C(19)–N(18)–C(2)–N(1)	177(3)
C(19)–N(18)–C(2)–N(3)	0(4)
C(2)–N(18)–C(19)–O(20)	3.0(4.0)
C(2)–N(18)–C(19)–O(21)	−179(2)
C(9)–C(4)–C(5)–C(10)	−180(2)
C(4)–C(5)–C(10)–O(11)	−33(3)
C(4)–C(5)–C(10)–C(12)	147(2)
C(6)–C(5)–C(10)–O(11)	148(2)
C(6)–C(5)–C(10)–C(12)	−32(3)
O(11)–C(10)–C(12)–C(13)	−12(3)
O(11)–C(10)–C(12)–C(17)	156(2)
C(5)–C(10)–C(12)–C(13)	169(2)
C(5)–C(10)–C(12)–C(17)	−23(3)
C(10)–C(12)–C(13)–C(14)	166(2)
C(10)–C(12)–C(17)–C(16)	−165(2)
O(20)–C(19)–O(21)–C(22)	1(4)
N(18)–C(19)–O(21)–C(22)	−180(2)

O(21) and C(6)–C(7). The query values of the aforementioned distances, also displayed in Table 2, are 1.216(11) and 1.341(11) Å, respectively. The mean values found in MOGUL were 1.340(15) (155 hits) and 1.383(21) (10,000 hits), respectively. The value of the C(19)–O(21) bond is typical of a C=O bond.[43] The O(20), which is connect by a double bond to the C(19) atom and also is intermolecularly connected by hydrogen bonds to atoms C(13) and N(3) may be the responsible for the abovementioned shorter bond, due to its strong acceptor-atom characteristic. In the case of C(6)–C(7) bond, the highest deviation from the least-squares plane passing through this 6-membered ring is 0.06(2) Å exactly for C(6) (r.m.s.e. of contributing atoms is 0.022 Å), thus decreasing the bond length.

Prior to the crystal structure determination of mebendazole form A presented herein, quantitative phase analyses (QPA) containing such a polymorph could not be carried out due to the lack of knowledge of its structure. QPA of one sample containing fractions of the polymorphs A and C[11] of mebendazole was performed here for the first time using X-ray powder diffraction, as far as we are concerned, as shown in Figure 7. A Rietveld refinement yielded the following goodness-of-fit indicators and R-factors, R_F^2, R_{wp}, and R_p, respectively: $\chi^2 = 6.615$, $R_F^2 = 3.44\%$, $R_{wp} = 7.45\%$, and $R_p = 5.67\%$. The structural parameters were kept fixed. Only the phase factors and terms that account for isotropic and anisotropic particle sizes were allowed to vary. For the major phase (form C), terms of anisotropic microstrain, as described by Stephens,[37] were also refined. The results indicated that the amounts of polymorphs A and C were, respectively, 3.7 and

Table 4. Intra(*) and Intermolecular Hydrogen Bonds of Mebendazole Form A

D–H···A	D–H (Å)	H···A (Å)	D···A (Å)	D–H···A (°)
N(3)–H(23)···O(20)*	1.00(7)	2.13(10)	2.69(3)	114(6)
N(3)–H(23)···O(11)[a]	1.00(7)	2. 30(8)	3.05(2)	131(7)
N(18)–H(32)···N(1)[b]	0.99(13)	2.09(14)	2.86(3)	133(11)
C(13)–H(27)···O(20)[a]	1.01(8)	2.39(8)	3.40(3)	175(6)

"D" and "A" are, respectively, hydrogen donor and acceptor.
*Intramolecular H bond.
[a]Symmetry: $-1-x$, $1-y$, $-z$.
[b]Symmetry: $-2-x$, $-y$, $-z$.

Table 5. 5-, 6-, and 9-Membered Rings Least-Squares Planes Calculations for Mebendazole Form A

N-Membered Rings	Most Deviating Atom(s)	Highest Deviation (Å)	r.m.s.e. (Å)
N(1)–C(8)–C(9)–N(3)–C(2)	C(8)	−0.08	0.022
C(4)–C(5)–C(6)–C(7)–C(8)–C(9)	C(6) and C(9)	0.06	0.022
C(12)–C(13)–C(14)–C(15)–C(16)–C(17)	C(16)	0.03	0.023
N(1)–C(8)–C(7)–C(6)–C(5)–C(4)–C(9)–N(3)–C(2)	N(1)	0.11	0.022

The most deviating atom of each ring with its subsequent highest deviation is also shown. r.m.s.e. means root mean square error of the contributing atoms.

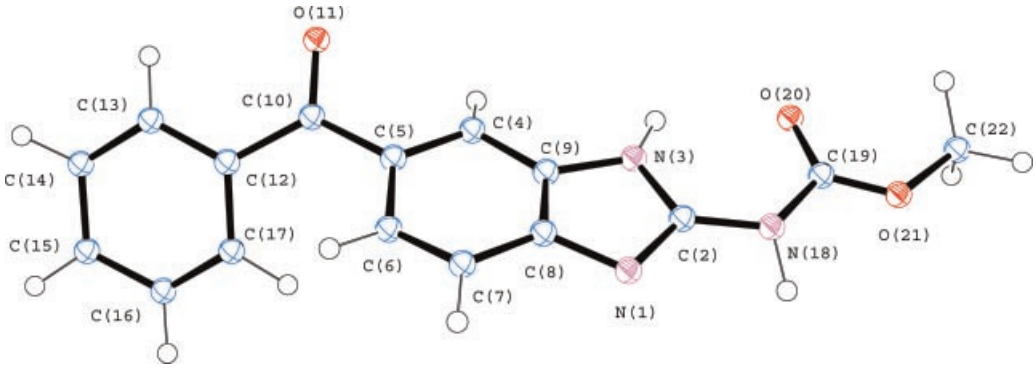

Figure 4. ORTEP-3[41] view of mebendazole form A showing the atoms labeling and 50% probability ellipsoids.

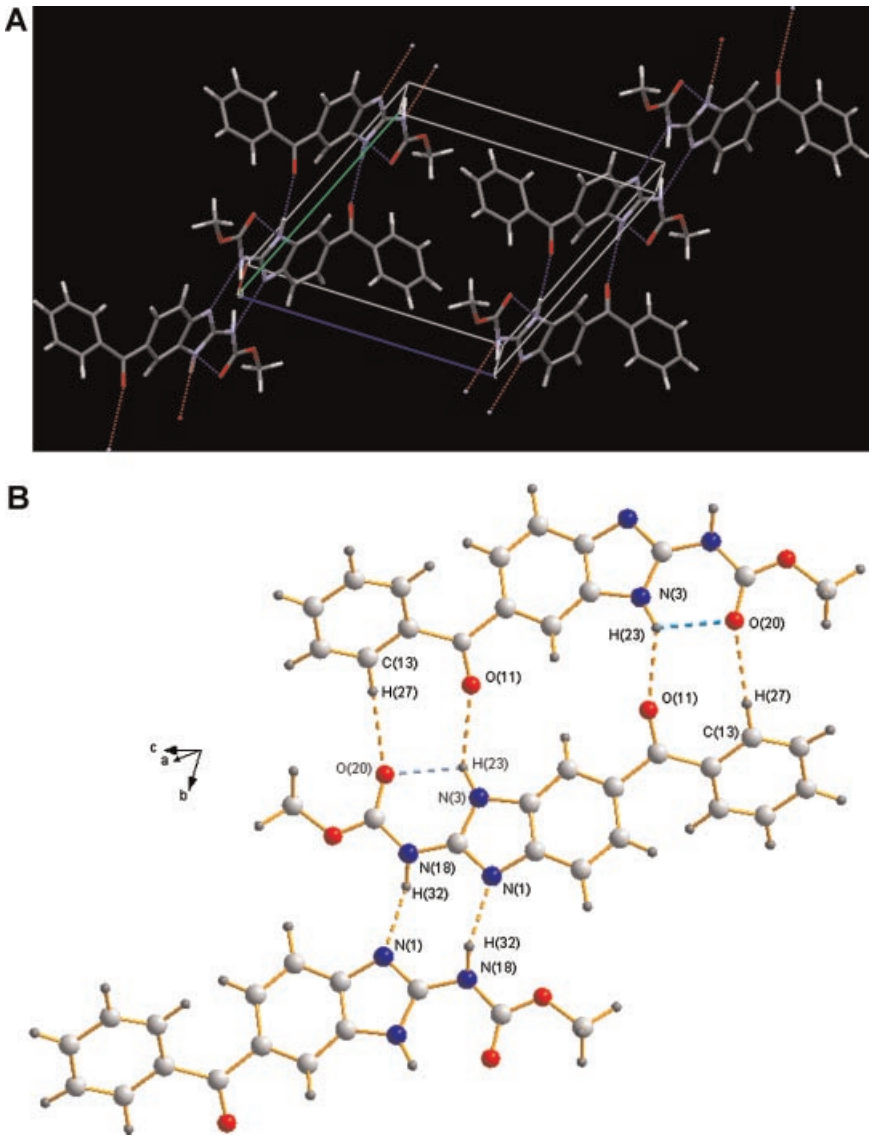

Figure 5. (a) Unit cell of mebendazole form A showing a section of an infinite chain along the (1 1 0) plane. (b) Intra- and intermolecular H-bonds of mebendazole form A.

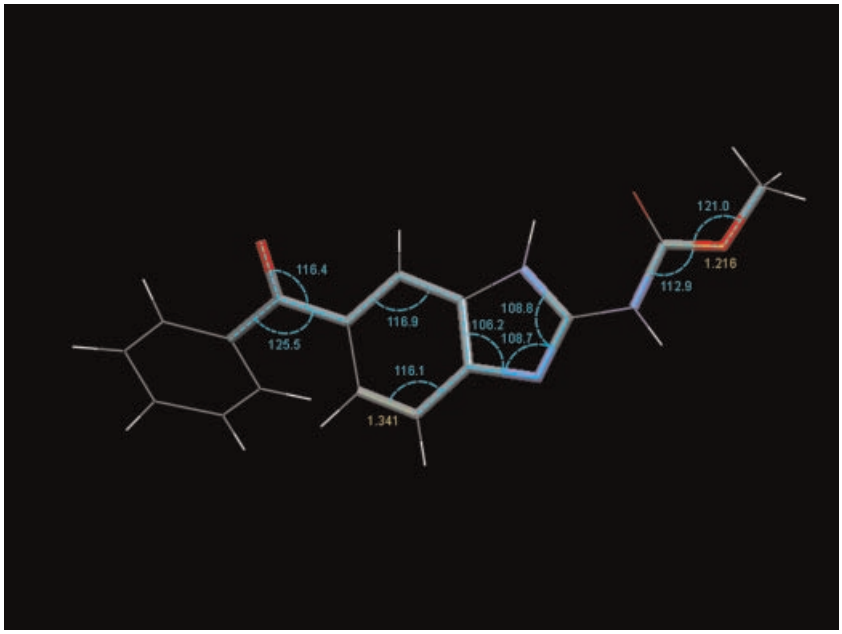

Figure 6. Details of bond distances and angles identified as "unusual" in MOGUL.

96.3 wt%. Although this small amount of form A does not degrade the final pharmaceutical product, correct evaluations of its presence can now be carried out.

In comparison with data obtained by other authors,[2,5,6,10,44] it is clearly seen that the use of high-resolution synchrotron X-ray powder diffraction data is of great importance in the process of structure determination of mebendazole form A, as well as many other substances, due to the minimization of peak superposition. What is more, there are no doubts that this polymorphic form of mebendazole was obtained as a single phase based both on the X-ray diffractograms depicted in Figures 3 and 7.

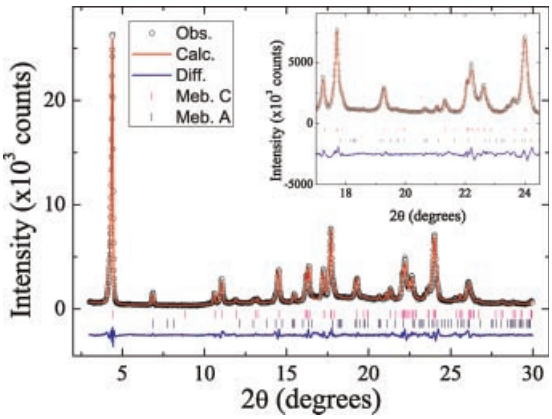

Figure 7. Rietveld plot of a sample containing both the polymorphs A and C of mebendazole used for quantitative phase analysis. Measured pattern (circles), calculated pattern (solid line), and difference profile (bottom solid line). Tick marks (|) at the bottom of the pattern indicate peak positions allowed by the unit-cell parameters and space groups of forms A and C. The inset presents a magnified region of the diffractogram.

CONCLUSIONS

The use of high-resolution synchrotron X-ray powder diffraction data, which minimized the peak superposition of the X-ray pattern, was used to determine the crystal structure of mebendazole form A. This pharmaceutical crystallizes under space group $P\bar{1}$. Quantitative phase analysis could be carried out for the first time by using the crystal structures of forms A and C of mebendazole. The phase fractions were 3.7 and 96.3 wt%, respectively. Although this small fraction of polymorph A does not degrade the final product, its presence must be correctly identified and quantified.

ACKNOWLEDGMENTS

We thank the financial support of FAPESP, CAPES, CNPq, and to the Brazilian Synchrotron Light Laboratory (LNLS) for beam time.

REFERENCES

1. Al-Badr AA, Tariq M. 1987. Analytical profiles of mebendazole. In: Florey K, editor. Analytical profiles of drug substances. New York: Academic Press. pp. 291–325.
2. Rodriguez-Caabeiro F, Criado-Fornelio A, Jimenez-Gonzalez A, Guzmán L, Igual A, Pérez A, Pujol M. 1987. Experimental chemotherapy and toxicity in mice of three mebendazole polymorphic forms. Chemotherapy 33:266–271.
3. Himmelreich M, Rawson BJ, Watson TR. 1977. Polymorphic forms of mebendazole. Aust J Pharm Sci 6:123–125.
4. Evans AC, Finscham JE, Dhamsay MA, Liebenberg W. 1999. Anthelmintic efficacy of mebendazole depends on molecular polymorph. S Afr Med J 89: 1118–1118.
5. Brusau EV, Camí GE, Narda GE, Cuffini S, Ayala AP, Ellena J. 2008. Synthesis and characterization of a new mebendazole salt: Mebendazole hydrochloride. J Pharm Sci 97:542–552.
6. Costa J, Fresno M, Guzmán L, Igual A, Oliva J, Vidal P, Pérez A, Pujol M. 1991. Polymorphic forms of mebendazole: Analytical aspects and toxicity. Cir Far 49:415–424.
7. Charoenlarp P, Waikagul J, Muennoo C, Srinophakun S, Kitayaporn D. 1993. Efficacy of single-dose mebendazole, polymorphic forms A and C, in the treatment of hookworm and Trichuris infections. J Trop Med Pub Health 24:712–716.
8. Swanepoel E, Liebenberg W, de Villiers MM. 2003. Quality evaluation of generic drugs by dissolution test: Changing the USP dissolution medium to distinguish between active and non-active mebendazole polymorphs. Eur J Pharm Biopharm 55:345–349.
9. Blaton NM, Peeters OM, De Ranter CJ. 1980. (5-benzoyl-1H-benzimidazol-2-yl)-carbamic acid methyl ester hydrobromide (mebendazole. HBr), $C_{16}H_{14}BrN_3O_3$. Cryst Struct Comm 9:181–186.
10. Caira MR, Dekker TG, Liebenberg W. 1998. Structure of a 1:1 complex between the anthelmintic drug mebendazole and propionic acid. J Chem Crystallogr 28:11–15.
11. Martins FT, Neves PP, Ellena J, Camí GE, Brusau EV, Narda GE. 2009. Intermolecular contacts influencing the conformational and geometric features of the pharmaceutically preferred mebendazole polymorph C. J Pharm Sci 98:2336–2344.
12. Aboul-Enein HY, Bunaciu AA, Fleschin S. 2002. Analysis of mebendazole polymorphs by Fourier transform IR spectrometry using chemometric methods. Biopolymers 67:56–60.
13. FDA. 2007. Guidance for Industry: ANDAs: Pharmaceutical Solid Polymorphism - Chemistry, Manufacturing, and Controls Information. ed., Rockville, MD: U.S. Department of Health and Human Services, Food and Drug Administration, Center for Drug Evaluation and Research (CDER).
14. David WIF, Shankland K, van de Streek J, Pidcock E, Motherwell WDS, Cole JC. 2006. DASH: A program for crystal structure determination from powder diffraction data. J Appl Crystallogr 39: 910–915.
15. Aarts E, Korst J. 1988. Simulated annealing and Boltzmann machines: A stochastic approach to combinatorial optimization and neural computing. Chichester, UK: John Wiley & Sons.
16. Van Laarhoven PJ, Aarts EH. 1987. Simulated annealing: Theory and applications. Dordrecht, Holland: Kluwer Academic Publishers.
17. Rietveld HM. 1969. A profile refinement method for nuclear and magnetic structures. J Appl Crystallogr 2:65–71.
18. Ferreira FF, Granado E, Carvalho W, Jr., Kycia SW, Bruno D, Droppa R, Jr. 2006. X-ray powder diffraction beamline at D10B of LNLS: Application to the Ba_2FeReO_6 double perovskite. J Synchrotron Radiat 13:46–53.
19. Giles C, Yokaichiya F, Kycia SW, Sampaio LC, Ardiles-Saravia DC, Franco MKK, Neuenschwander RT. 2003. High-resolution X-ray diffraction beamline at the LNLS for the study of charge, orbital and magnetic structures. J Synchrotron Radiat 10:430–434.
20. Rodrigues R. 2004. Polimorfismo do Mebendazol. Formil Química Ltda. Private Communication. Jandira, SP, Brazil.
21. Boultif A, Louër D. 1991. Indexing of powder diffraction patterns for low-symmetry lattices by the successive dichotomy method. J Appl Crystallogr 24:987–993.
22. Toby BH. 2005. CMPR—A powder diffraction toolkit. J Appl Crystallogr 38:1040–1041.
23. Shirley R, Louër D. 1978. New powder indexing programs for any symmetry which combine grid-search with successive dichotomy. Acta Crystallogr A 34:S382.
24. Shirley R. 2002. The Crysfire 2002 system for automatic powder indexing: User's manual. Version 4.06. GuildFord Surrey, England: The Lattice Press.
25. de Wolff PM. 1968. A simplified criterion for the reliability of a powder pattern indexing. J Appl Crystallogr 1:108–113.
26. Kohlbeck F, Hörl EM. 1978. Trial and error indexing program for powder patterns of monoclinic substances. J Appl Crystallogr 11:60–61.
27. Hahn T. 1983. International tables for crystallography. 1st edition. Dordrecht, Holland: The International Union of Crystallography. p. 871.
28. Pawley GS. 1981. Unit-cell refinement from powder diffraction scans. J Appl Crystallogr 14:357–361.
29. Wishart DS, Knox C, Guo AC, Shrivastava S, Hassanali M, Stothard P, Chang Z, Woolsey J. 2006.

DrugBank: A comprehensive resource for in silico drug discovery and exploration. Nucleic Acids Res 34:D668–D672.
30. Spek AL. 2003. Single-crystal structure validation with the program PLATON. J Appl Crystallogr 36: 7–13.
31. Krivý I, Gruber B. 1976. A unified algorithm for determining the reduced (Niggli) cell. Acta Crystallogr A 32:297–298.
32. Larson AC, Von Dreele RB. 2001. General Structure Analysis System (GSAS) (Report LAUR 86-748). Los Alamos, NM: Los Alamos National Laboratory.
33. Toby BH. 2001. EXPGUI, a graphical user interface for GSAS. J Appl Crystallogr 34:210–213.
34. Le Bail A, Duroy H, Fourquet JL. 1988. Ab-initio structure determination of $LiSbWO_6$ by X-ray powder diffraction. Mater Res Bull 23:447–452.
35. Thompson P, Cox DE, Hastings JB. 1987. Rietveld refinement of Debye-Scherrer synchrotron X-ray data from Al_2O_3. J Appl Crystallogr 20:79–83.
36. Finger LW, Cox DE, Jephcoat AP. 1994. A correction for powder diffraction peak asymmetry due to axial divergence. J Appl Crystallogr 27:892–900.
37. Stephens PW. 1999. Phenomenological model of anisotropic peak broadening in powder diffraction. J Appl Crystallogr 32:281–289.
38. Wright J. 1998. Using the "Plab" (PerL Angles and Bonds) Perl script by Jon Wright for generating bond length and angle restraints macros for GSAS on organic structures. ed.
39. Toby BH. 2006. R factors in Rietveld analysis: How good is good enough? Powder Diffr 21:67–70.
40. Hill RJ, Flack HD. 1987. The use of the Durbin-Watson d statistic in Rietveld analysis. J Appl Crystallogr 20:356–361.
41. Farrugia LJ. 1997. ORTEP-3 for Windows—A version of ORTEP-III with a Graphical User Interface (GUI). J Appl Crystallogr 30:565–565.
42. Bruno IJ, Cole JC, Kessler M, Luo J, Sam Motherwell WD, Purkis LH, Smith BR, Taylor R, Cooper RI, Harris SE, Orpen AG. 2004. Retrieval of crystallographically-derived molecular geometry information. J Chem Inf Comp Sci 44:2133–2144.
43. Schultheiss N, Newman A. 2009. Pharmaceutical cocrystals and their physicochemical properties. Cryst Growth Des 9:2950–2967.
44. Swanepoel E, Liebenberg W, Devarakonda B, de Villiers MM. 2003. Developing a discriminating dissolution test for three mebendazole polymorphs based on solubility differences. Pharmazie 58:117–121.